Available online at www.sciencedirect.com
SCIENCE DIRECT®
Pergamon
Cement and Concrete Research 34 (2004) 157–164
CEMENT AND CONCRETE RESEARCH

Magnesia–ammonium phosphate-bonded cordierite refractory castables: Phase evolution on heating and mechanical properties

Nora E. Hipedinger*, Alberto N. Scian, Esteban F. Aglietti

CETMIC: Centro de Tecnología de Recursos Minerales y Cerámica (CIC-CONICET-UNLP), C.C. No. 49, (B1897ZCA) Manuel B. Gonnet, Provincia de Buenos Aires, Argentina

Received 23 January 2003; accepted 18 July 2003

Abstract

A cordierite refractory castable was developed using the MgO-$NH_4H_2PO_4$ reaction. This castable was made with cordierite–mullite aggregates from scrap refractory material and a cement paste based on magnesia, calcined alumina, silica fume, and ammonium dihydrogen phosphate, which forms cordierite ($2MgO{\cdot}2Al_2O_3{\cdot}5SiO_2$) during heating at high temperature. The mix with water was cast into steel molds; the cold setting occurs within 30 min. The set castables were thermally treated and the evolution of the phases was observed. Struvite ($NH_4{\cdot}MgPO_4{\cdot}6H_2O$) was identified at room temperature; between 110 and 750 °C, the present phosphates were amorphous to X-ray diffraction (XRD). At 1100 °C, magnesium orthophosphate ($Mg_3(PO_4)_2$) and aluminum orthophosphate ($AlPO_4$) were present. At 1350 °C, the main crystalline phases were cordierite and mullite. Cold and hot flexural strength, thermal shock resistance, and physical properties were measured. The properties of magnesia–phosphate-bonded cordierite castables were compared with cordierite material obtained by conventional slip-casting method from aggregates, clay, talc, and calcined alumina.

Keywords: Chemically bonded ceramics; Refractory cement; Magnesia–phosphate cement; MgO; Composite

1. Introduction

Materials based on cordierite ($2MgO{\cdot}2Al_2O_3{\cdot}5SiO_2$) are best suited to applications that require low thermal expansion coefficient (2×10^{-6} °C^{-1} to 6×10^{-6} °C^{-1}) and outstanding thermal shock resistance. These materials are extensively used as refractory products (kiln furniture, saggers, gas burners), electroceramics (resistors, fusibles, flame guards), tableware (flame-proof applications as cooking ware, laboratory items), and catalyst carriers. The low intrinsic strength of cordierite can be somehow compensated by the presence of mullite ($3Al_2O_3{\cdot}2SiO_2$) in spite of some increase in the thermal expansion coefficient results. Mullite by itself is an excellent refractory material with good thermal shock resistance and it has a thermal expansion coefficient of about 5.4×10^{-6} °C^{-1}. Then, the cordierite–mullite composite materials exhibit high thermal and mechanical strength at service temperatures below 1300 °C.

Since few natural deposits of cordierite exist, a stable cordieritic material can be easily obtained from economical raw materials that contain silica, magnesia, and alumina in suitable proportions. Compounds such as oxides, carbonates, and hydroxides and minerals such as kaolin, clay, talc, sepiolite, steatite, and chlorite can be utilized. The magnesia is seldom used as a raw material because the reaction to form cordierite with the other compounds takes a long time to be completed. Refractory bodies with high contents of cordierite are commonly made from a mix of talc and plastic clay; alumina additions are often used [1,2]. This mix is then pressed, rammed, cast, extruded, etc., producing cordierite-based bodies during heating at high temperature. The overheating of these bodies produces some decomposition of the cordierite that results in the formation of small amounts of spinel and mullite. Additions of $ZrSiO_4$, $MgCO_3$, $BaCO_3$, $PbSiO_3$, SiC, graphite, silica fume, and other mineralizers had been investigated [3,4]. Besides the nature of the raw materials used, the synthesis of cordierite is also influenced by the initial structural state of the respective reactant, by the presence or absence of

* Corresponding author. Tel.: +54-221-484-0247; fax: +54-221-471-0075.
E-mail address: norahipe@ing.unlp.edu.ar (N.E. Hipedinger).

0008-8846/$ – see front matter © 2003 Elsevier Ltd. All rights reserved.
doi:10.1016/S0008-8846(03)00256-4

impurities, and by the composition, area, and size of the grains [5–7].

Refractory cordierite materials are based on a matrix consisting of cordierite or cordierite–mullite as major components and aggregates of different compositions and sizes such as calcined flint, tabular alumina, and low and high mullite content aggregates. Suitable aggregate size distribution is required to obtain materials with the best service properties (density, strength, expansion, etc.), depending also on the application or the installation method employed.

The bonding properties of a large number of phosphate materials have been recognized for many years [8–11]. Numerous processes for the utilization of these properties have been patented, and both heat- and cold-setting compositions have been described. Phosphate bonds are usually employed in dental cements, rapid-setting cements recommended for repair work and refractories. They are of particular interest in the field of refractories because of the high fusion temperature of many phosphates that allow to design chemically bonded refractories. Magnesia–phosphate cement (MPC) is one of most employed for quick-setting and high early strength requirements, specially for rapid repairs of damaged concrete roads, motorways, bridge decks, airfields, manhole raising, industrial floors, and any other type of application where time is one of the main considerations [12,13].

The characteristic reaction of MPC-based materials is an acid–base reaction or, more precisely, the reaction between certain magnesium compounds and phosphates usually in aqueous solution. Due to their setting properties, in most cases, the compounds used are dead-burnt magnesia and acid ammonium phosphates, particularly ammonium dihydrogen phosphate ($NH_4H_2PO_4$) [14–25]. Diammonium hydrogen phosphate ($(NH_4)_2HPO_4$), ammonium polyphosphate, monoaluminum phosphate ($Al(H_2PO_4)_3$), and orthophosphoric acid (H_3PO_4) have also been utilized [19,26–32]. An exothermic reaction takes place when the reagents are put in contact and the reaction product, usually a hydrated salt or a hydrogel, forms the cement matrix in which the fillers are embedded. Magnesia with low superficial reactivity is required to avoid a violent reaction. Magnesia is generally present in excess in the hydrated pastes. The hydration of MPC is complex because the presence of several overlapping reactions and different reaction paths, depending moreover of the others phases present and the experimental variables. The hydration reactions can be controlled and modified by the use of retarders to achieve a suitable long setting time, while the commercially available mortars contain various types and grades of fillers.

This paper is about the preparation, characterization, and comparison of two cordierite refractory castables: one by the conventional slip-casting method utilizing talc, clay, and alumina, and the other employing the $MgO\text{-}NH_4H_2PO_4$ setting reaction.

2. Experimental

2.1. Materials and preparation method

Two kinds of refractory castables, which form cordierite on heating at high temperature, were prepared. Both castables were designed with 40 wt.% of fine fraction (matrix) and 60 wt.% of coarse fraction (aggregates). The aggregates, named A, were the same for both castables and they came from kiln furniture scrap of the ceramic industry. They were cordierite–mullite grains with adequate grain size distribution from mesh 8 up to 50 (ASTM).

The castables designated by ATW (aggregate–talc–water) were obtained by the conventional method of slip casting, with the A aggregates and a matrix named T containing talc, clay, and calcined alumina in the right proportions to obtain the stoichiometric cordierite composition on heating (13.7% MgO, 34.9% Al_2O_3, and 51.4% SiO_2). These solids were mixed with water (W), cast in plaster molds of $25 \times 25 \times 150$ mm^3, and air dried at room temperature for several days.

A commercial pure talc, mesh 325, was employed (origin China). The crystalline phases observed by X-ray diffraction (XRD) were talc ($3MgO{\cdot}4SiO_2{\cdot}H_2O$) and magnesite ($MgCO_3$).

The clay (Tincar Super, Piedra Grande, Argentine) had a specific surface area (BET) of 23 $m^2\ g^{-1}$. The percentage retained in mesh 150 and 325 was 1% and 2%, respectively. The main mineralogical phases were quartz (SiO_2) and kaolinite. The chemical analyses of the clay and talc are shown in Table 1.

The alumina (Al_2O_3) was of a calcined type (S3G, Alcan) with a mean particle size of 5 μm, a specific surface area (BET) of 1 $m^2\ g^{-1}$, and 0.49% of Na_2O. The crystalline phases of calcined alumina were α-Al_2O_3 and impurities of sodium aluminum oxide (β-$NaAl_{11}O_{17}$).

The chemical bond magnesia–phosphate was taken into account to design the other castable named AMP (aggregate–magnesia–phosphate). This castable was prepared with the A aggregates mentioned above and a matrix, named M, formulated with magnesia, silica fume, and calcined alumina in the proportions of the theoretical cordierite composition.

The magnesia employed (MgO) was of refractory grade with a particle size <75 μm. The specific surface area was 0.35 $m^2\ g^{-1}$ and the density was 3.59 g cm^{-3} (by pycnometry). The chemical analysis is reported in Table 1.

Table 1
Chemical analyses of raw materials (wt.%)

Raw material	SiO_2	Al_2O_3	Fe_2O_3	CaO	MgO	Na_2O	K_2O	TiO_2	LOI 1000 °C
Clay	64.37	22.69	1.14	0.20	0.20	0.47	0.65	0.53	8.77
Talc	59.94	0.15	0.52	0.60	30.44	0.27	<0.01	<0.01	7.30
Magnesia	2.95	0.19	0.70	1.97	93.28	0.46	<0.01	0.02	<0.01

Periclase (MgO) and traces of $CaMgSiO_4$ (monticellite), Mg_2SiO_4 (forsterite), and $MgAl_2O_4$ were the crystalline phases. Before preparing the castables, magnesia was calcined for 1 h at 1000 °C to eliminate the carbonates and superficial hydrates.

The SiO_2 used was silica fume EMS 965 from Elkem Materials. It was observed that the silica fume was amorphous at low temperatures, and at temperatures higher than 1000 °C, it crystallized in cristobalite and tridymite form. Silicon carbide (SiC) was present as impurity in the silica fume.

The calcined alumina used in M matrix was the same as that of the T matrix.

The dry-mixed solids (M matrix and A aggregates) were bonded with an aqueous solution of ammonium dihydrogen phosphate ($NH_4H_2PO_4$), supplied by J.T.Baker, named P. The solution was 28 wt.% on the basis of solid mix to obtain a good consistency. The $MgO/NH_4H_2PO_4$ molar ratio was 2.3. The solution P was added to solids following the normal procedure in the construction industry. A workable paste was obtained with vigorous mixing, in a Hobart-type mixer, for about 2 min. The paste was poured in metallic molds of $25 \times 25 \times 150$ mm^3 and then was vibrated for 1 min. The probes remained 24 h at room temperature (about 20 °C) and then they were removed from the molds and air dried 24 h more at room temperature.

Then, both AMP and ATW castables were air dried at 110 °C for 24 h and heated at 600, 750, 1100, and 1350 °C for 2 h in an electric furnace in air atmosphere.

2.2. Test methods

The XRD patterns were obtained using a Philips PW-3710 diffractometer with Cu-Kα radiation ($\lambda = 0.154$ nm) at 40 kV and 20 mA (step size: 0.02 °2θ; time per step: 1 s).

Dilatometric analyses of the castables were performed in a Netzsch apparatus with a heating rate of 5 °C min^{-1} in specimens of $10 \times 10 \times 50$ mm^3.

The flexural strength was evaluated through the cold modulus of rupture (CMOR) and the hot modulus of rupture (HMOR). CMOR was measured using a T22K-type equipment from J. J. Lloyd Instruments Limited (UK). HMOR was measured at 1200 °C in a Netzsch equipment, 422 model, at constant load rate (9 MPa min^{-1}). Before testing, the probes were heated at 10 °C min^{-1} up to 700 °C, then at 5 °C min^{-1} from 700 to 1200 °C, and maintained at 1200 °C for 15 min.

Thermal shock resistance test was based on the loss of flexural strength after heating–cooling cycles. The castables, previously calcined at 1350 °C for 2 h, were heated at 1000 °C for 1 h and then they were rapidly cooled by water immersion at 20 °C. After three cycles of heating–cooling, the CMOR was measured.

The pore size distribution was examined by means of two Carlo Erba mercury porosimeters: Porosimeter 2000 and Macropores unit 120.

The open porosity was determined by the Arquimedes method (ASTM C-20).

3. Results and discussion

3.1. Physical and textural properties

Table 2 shows some properties of the AMP and ATW castables calcined at 1350 °C. The linear change between 110 and 1350 °C showed a small contraction for the AMP castable and a small expansion for the ATW castable. The low density of both castables was expected because of the high porosity (around 30%) of the A aggregates (scrap). The thermal expansion coefficient of ATW castable was smaller than that of the AMP castable, but both materials had a good behavior during the thermal shock test. The ATW castable showed a higher open porosity and a higher cumulative volume of macro- and micropores than AMP castable, which affected their mechanical properties.

Fig. 1 shows the dilatometric curves of the ATW and AMP castables dried at 110 °C. For the AMP castable, a small expansion up to 1100 °C was observed. At this temperature, a considerable shrinkage began reaching 1.95% at 1350 °C, which indicates that this calcination temperature was too high for this kind of material. The addition of phosphates reduces refractoriness due to the formation of liquid phases, probably magnesium metaphosphate ($MgO \cdot P_2O_5$, melting point 1165 °C) and compounds of the SiO_2-P_2O_5 system. At ordinary temperatures, the silica does not react with the phosphates and it does not produce phosphorus compounds with bonding properties. At temperatures between 1100 and 1300 °C, liquid phases ($SiO_2 \cdot P_2O_5$ and $2SiO_2 \cdot P_2O_5$) not desirable for refractory materials are formed. This phosphate bond is suitable for moderate heat duty refractories when a cold setting is desired. The ATW castable showed an expansion of only 0.15% during heating up to 1350 °C. The absence of phosphate compounds in this castable produced a minor amount of liquid phases.

In Fig. 2, the linear changes of the ATW castable calcined for 2 h at 1350 °C and the AMP castables calcined

Table 2
Physical and textural properties of the AMP and ATW castables calcined for 2 h at 1350 °C

	AMP	ATW
Linear change 110–1350 °C (%)	−0.54	0.55
Apparent density (g cm^{-3})	1.7	1.8
Thermal expansion coefficient at 25–1000 °C (°C^{-1}) ($\times 10^{-6}$)	2.3	1.3
Open porosity (%)	29.7	32.4
Cumulative macropores volume between 1.8 and 30.5 μm (mm^3 g^{-1})	132.3	167.0
Cumulative micropores volume between 0.0036 and 6.5 μm (mm^3 g^{-1})	97.8	189.1

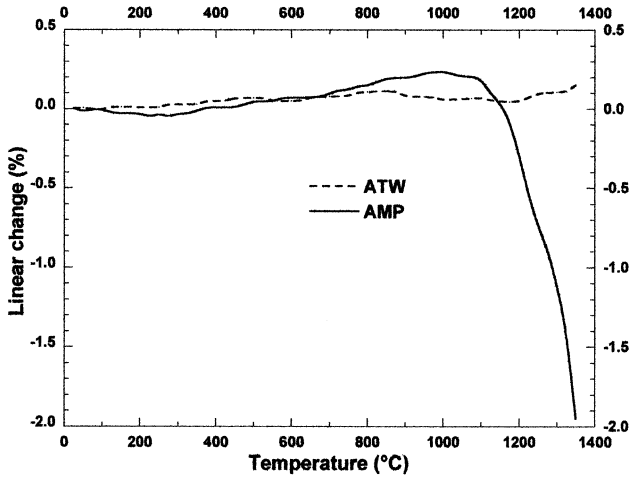

Fig. 1. Dilatometry of the AMP and ATW castables dried at 110 °C.

for 2 h at 1100 and 1350 °C from dilatometric tests are shown. The ATW castable had the smallest thermal expansion coefficient and a linear change of 0.25% up to 1350 °C. The AMP castable calcined at 1350 °C began to shrink at 1300 °C, indicating that the service temperature for this kind of material should not exceed 1250 °C. The AMP castable heated at 1100 °C had a thermal expansion coefficient of 3.8×10^{-6} °C^{-1} between 25 and 1000 °C, slightly higher than the ATW and AMP coefficients at 1350 °C because the matrix had still not transformed into cordierite at 1100 °C; anyway, the cordierite–mullite aggregates contributed to reach a good thermal expansion coefficient.

3.2. Evolution of the phases on heating

Fig. 3 shows the crystalline phases present in the A aggregates, the T matrix, and the ATW castables after heating 24 h at 110 °C and 2 h at 1100 and 1350 °C. The main crystalline phases of the A aggregates were cordierite ($2MgO{\cdot}2Al_2O_3{\cdot}5SiO_2$) and mullite ($3Al_2O_3{\cdot}2SiO_2$); the minor crystalline phases were alumina (Al_2O_3), magnesia (MgO), quartz (SiO_2), and spinel ($MgO{\cdot}Al_2O_3$).

The XRD pattern of the T matrix showed the presence of talc ($3MgO{\cdot}4SiO_2{\cdot}H_2O$), kaolinite, and quartz coming from clay, alumina, and impurities of magnesite ($MgCO_3$) coming from the talc and sodium aluminum oxide (β-$NaAl_{11}O_{17}$) coming from the alumina.

The diffractogram of castable dried 24 h at 110 °C (ATW 110 °C) showed the crystalline phases of the A aggregate plus the T matrix.

At 750 °C (XRD pattern not shown in Fig. 3), the clay and the magnesite were completely decomposed and the talc was partially dissociated.

At 1100 °C (XRD pattern ATW 1100 °C), the T matrix began to transform into mullite and cordierite. The quartz and the silica coming from the talc and clay decomposition became cristobalite. Besides cordierite and mullite coming from the aggregates, alumina, protoenstatite ($MgO{\cdot}SiO_2$), and small amounts of talc and spinel were also present.

At 1350 °C (XRD pattern ATW 1350 °C), the final phases were cordierite and mullite, accompanied by small amounts of spinel, alumina, magnesia, and cristobalite. The crystalline phase $2MgO{\cdot}2Al_2O_3{\cdot}5SiO_2$ is referred for simplification by the general term "cordierite"; however, the term "indialite" would be more appropriate to designate the hexagonal form initially present in cordierite refractory bodies. The transformation into the orthorhombic form, cordierite, takes place only after prolonged heating.

MPCs are important in refractory bonding systems. Then it is essential to understand the phase changes that occur on heating. Fig. 4 shows the XRD pattern of the A aggregate, the M matrix, and the AMP phosphate-bonded castable after remaining 48 h at room temperature (around 20 °C), drying 24 h at 110 °C, and heating 2 h at 1100 and 1350 °C.

The A aggregates were the same that the ones used in the ATW castables; consequently, cordierite and mullite were the main crystalline phases.

XRD pattern of the M matrix (constituted by magnesia, alumina, and silica fume) showed alumina and magnesia as predominant phases. A broad hump in the background of the diffractogram, about 22° of 2θ, was also observed indicating the presence of amorphous silica. Very small quantities of sodium aluminum oxide (β-$NaAl_{11}O_{17}$) and silicon carbide (SiC), coming from calcined alumina and silica fume, respectively, were also present.

The diffractogram of AMP castable set at room temperature (XRD pattern AMP 20 °C) showed the reflections of cordierite–mullite corresponding to the A aggregate, as well as alumina, magnesia, and amorphous silica coming from the M matrix. Ammonium magnesium phosphate hexahydrate ($NH_4MgPO_4{\cdot}6H_2O$), called struvite, was formed as reaction product among MgO, $NH_4H_2PO_4$, and H_2O at room temperature. Studies of the hydration of magnesia–

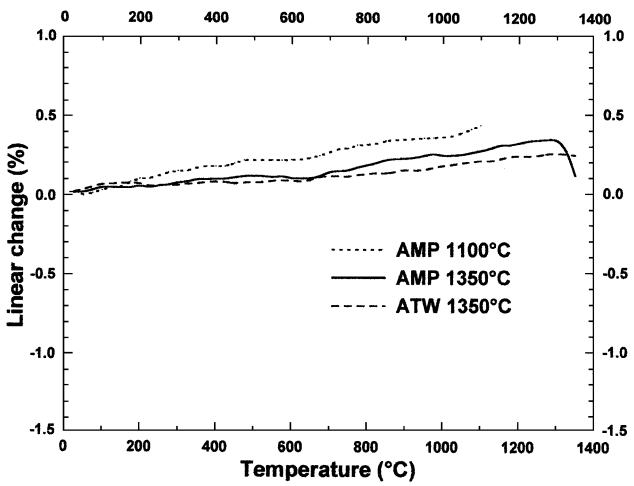

Fig. 2. Linear change of the ATW castable calcined for 2 h at 1350 °C and the AMP castables calcined for 2 h at 1100 and 1350 °C.

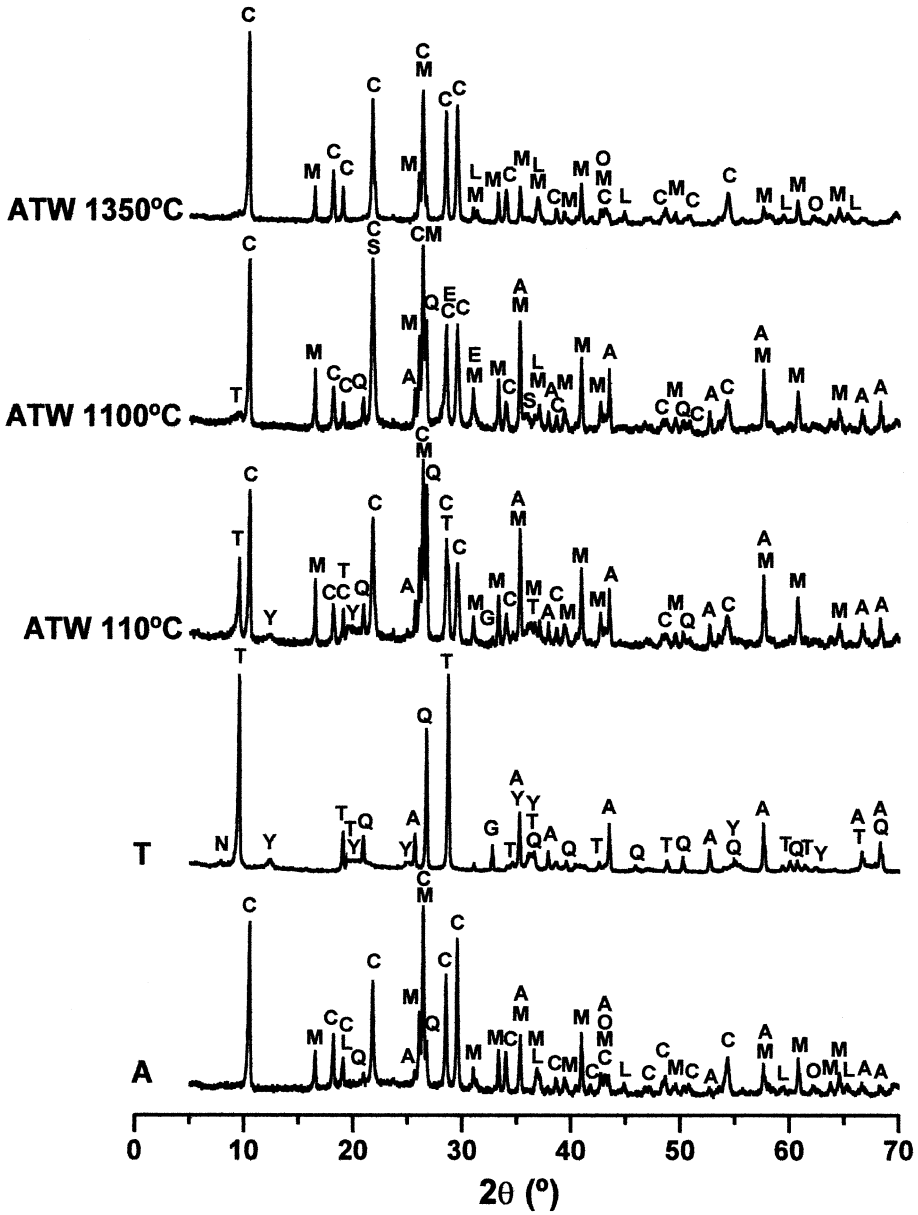

Fig. 3. XRD pattern of the aggregate (A), the matrix (T), and the castable (ATW) at different temperatures. C = cordierite, M = mullite, A = alumina, T = talc, Y = clay, G = magnesite, O = magnesia, E = protoenstatite, L = spinel, Q = quartz, S = cristobalite, N = sodium aluminum oxide.

ammonium dihydrogen phosphate–water mix [12] indicated the presence of an amorphous phase during the first hour of setting, which gradually crystallized to struvite. The reaction mechanism proposed initially involved the formation of amorphous colloidal-type particles composed of hydrogen-bonded water, ammonium dihydrogen phosphate, and a multimolecular struvite framework. Afterwards, these particles coagulated around excess magnesia and aggregates to start setting. During setting and drying, crystalline struvite was formed. In this study, other ammonium magnesium phosphate hydrates, as schertelite ($(NH_4)_2Mg(HPO_4)_2 \cdot 4H_2O$) and dittmarite ($NH_4MgPO_4 \cdot H_2O$), were not detected in the diffractograms after 48 h from the preparation, probably because the hydration was completed and because the water was not the limiting reagent. The presence of amorphous phases containing magnesium was also suggested. The exact amount of magnesium that formed struvite, amorphous phase, or magnesia unreacted depends on a number of factors, such as the molar ratio $MgO/NH_4H_2PO_4$, the particle size and reactivity of the starting materials, and the intimacy and duration of mixing. At low temperatures, the alumina practically did not react with the ammonium dihydrogen phosphate solution.

In the castable dried at 110 °C (XRD pattern AMP 110 °C), struvite was not present and a higher background in angles below 25° 2θ was observed. Also, a smell of ammonia was noticed during drying. These facts suggested that struvite decomposed at around 110 °C, evolv-

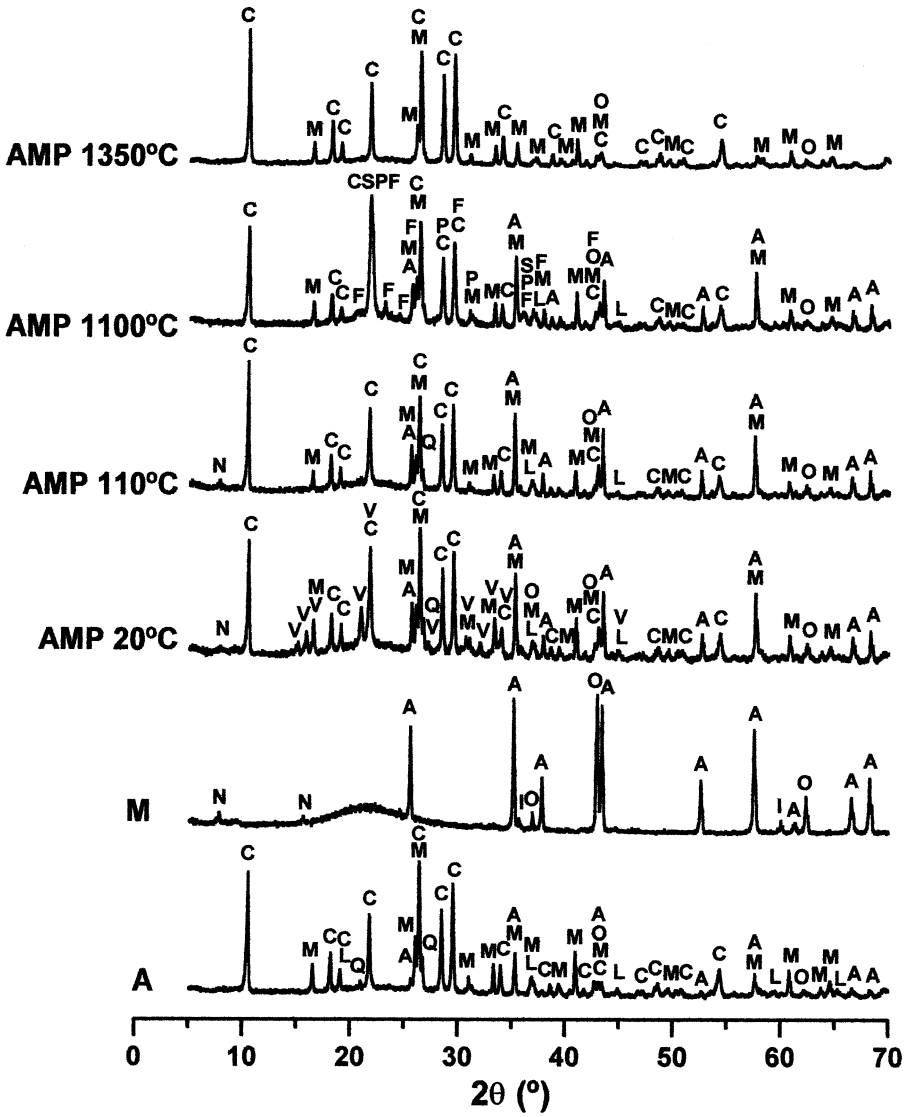

Fig. 4. XRD pattern of the aggregate (A), the matrix (M), and the castable (AMP) at different temperatures. C = cordierite, M = mullite, A = alumina, O = magnesia, V = struvite, F = farringtonite, P = aluminum orthophosphate, L = spinel, Q = quartz, S = cristobalite, I = silicon carbide, N = sodium aluminum oxide.

ing ammonia and water and generating a noncrystalline compound.

The diffractograms at 450 and 600 °C (not shown in Fig. 4) were identical to those at 110 °C. The XRD pattern of the castable at 750 °C (not shown) indicated that the phosphates of the amorphous phase began to crystallize as magnesium orthophosphate or farringtonite ($Mg_3(PO_4)_2$). In experiences carried out with the cement paste alone (without aggregates), at 750 °C, the presence of magnesium pyrophosphate ($Mg_2P_2O_7$), besides farringtonite, was observed, in agreement with that reported by Abdelrazig et al. [15–17].

At 1100 °C (XRD pattern AMP 1100 °C), an intense reflection at 21.8° of 2θ was observed, corresponding to the transformation of the amorphous silica of the matrix into cristobalite and to the formation of the aluminum orthophosphate ($AlPO_4$, cristobalite form). Aluminum orthophosphate resembles silica in structure having the same polymorphic transformations. Small amounts of farringtonite were also present at 1100 °C.

At 1350 °C (XRD pattern AMP 1350 °C), the transformation of the phases into cordierite was observed, intensifying the cordierite reflections coming from the aggregates. At this temperature, the alumina was thoroughly consumed and small amounts of farringtonite, spinel, and unreacted magnesia were detected. The almost total absence of crystalline phosphate phases suggested that the phosphates were present in the glassy phase. There was no evidence for the decomposition of the material producing P_2O_5 since there was practically no loss in mass on heating between 800 and 1350 °C.

Comparing the XRD patterns at 1350 °C of the ATW and AMP castables (Figs. 3 and 4, respectively), it was observed

Table 3
CMOR after thermal treatment at different temperatures and after three cycles of thermal shock, and HMOR of the ATW and AMP castables

	AMP	ATW
CMOR (MPa)		
20 °C, 48 h	1.3	–
110 °C, 24 h	1.3	0.6
600 °C, 2 h	1.1	–
1100 °C, 2 h	2.6	3.8
1350 °C, 2 h	13.4	8.1
After thermal shock[a]	5.3	5.4
HMOR (MPa)		
1200 °C, 15 min[b]	14.0	8.1

[a] Probes previously calcined 2 h at 1350 °C and submitted to three cycles of heating–cooling ($\Delta T \cong 1000$ °C).
[b] Probes previously calcined 2 h at 1350 °C.

that the crystalline phases were practically the same, except for a slightly higher content of mullite and spinel in ATW castable. In turn, these diffractograms were very similar to the XRD pattern of the aggregate, except for the presence of quartz in the last one. Therefore, the conventional method (ATW castables) and the magnesia–phosphate bond method (AMP castables) produce cordierite–mullite composite materials with similar crystalline phases. The main advantage of AMP castables is based on its cold and rapid setting, where the time is measured in hours instead of days, which leads to a shorter time of process and to a more efficient use of the molds. The AMP castables set after around 30 min and hardened after several hours. The setting time can be adjusted to the time required, depending on the application, selecting the suitable type of magnesia (specially the superficial reactivity), phosphate concentration, magnesia/phosphate ratio, and retarders.

3.3. Mechanical properties

The mechanical behavior of the AMP and ATW castables was evaluated measuring the CMOR and HMOR. Table 3 shows the CMOR of both castables after 48 h (starting from the preparation) at 20 °C, 24 h at 110 °C, 2 h at 600, 1100 and 1350 °C and after three cycles of heating–cooling (thermal shock), and the HMOR at 1200 °C. Up to 600 °C the CMOR values of the AMP castables were similar, near 1.3 MPa. Although this value was low, it was twice the value obtained for ATW castable (0.6 MPa) and it was enough to transport and manipulate the materials formed. Crystalline and amorphous hydrated magnesium/ammonium phosphates, coming from the $MgO\text{-}NH_4H_2PO_4$ chemical bond, contributed to the strength of the AMP castables at low temperatures. Increasing the temperature, a heat setting occurred, similar to that observed in the commercial phosphate refractories. The smaller CMOR value at 1100 °C of the AMP castable (2.6 MPa) compared with the ATW castable (3.8 MPa) is probably due to the presence of aluminum or magnesium orthophosphate. At 1350 °C, although both castables presented similar crystalline phases and the ATW castable had even a slightly higher content of mullite, the CMOR value of the AMP castable was 40% higher than that of the ATW castable (13.4 and 8.1 MPa, respectively). This is surely due to the higher glass content and the lower porosity (mainly macropores) of the AMP castable. The CMOR values obtained for both castables can be related to the low density and high porosity of the aggregate grains (cordierite–mullite) employed. High water/solid ratio was utilized because most of the water was necessary to fill the pores. So, if low porosity or dense aggregates were used, the mechanical strength could be improved.

The thermal shock resistance of the castables calcined at 1350 °C was evaluated through the loss of the CMOR after three cycles of heating at 1000 °C and quenching in cold water ($\Delta T \cong 1000$ °C in few seconds). After this test, both castables showed practically the same CMOR value (near 5.4 MPa), but the CMOR had decreased 33% for the ATW castable and 60% for the AMP castable, in agreement with the higher level of vitrification of the latter. The thermal shock resistance of both castables was good, taking into account the severity of the test and that the calcination temperature of 1350 °C was too high for the phosphate-bonded castables.

The HMOR value at 1200 °C of the ATW castable, previously calcined 2 h at 1350 °C, was identical to the CMOR value (8.1 MPa). The HMOR value of the AMP castable (14.0 MPa) was slightly higher than the CMOR value attributable to the release of the internal stress of the material, the suppression of cracks, and/or the accommodation of the microstructure.

Fig. 5 shows the load-deflection curve, obtained at constant temperature of 1200 °C and constant load rate for both castables previously calcined 2 h at 1350 °C. The AMP castable supported considerably higher loads than the ATW castable, although the final deflection up to fracture was practically the same for both castables. No plastic deformation was observed.

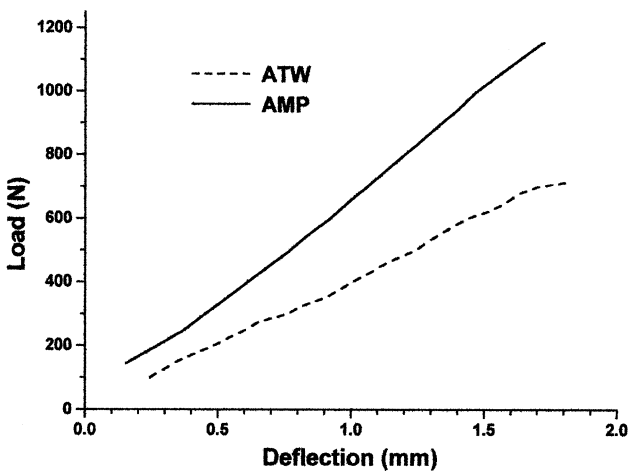

Fig. 5. Load-deflection curve up to the fracture, at 1200 °C, for the AMP and ATW castables (previously calcined for 2 h at 1350 °C).

4. Conclusions

Cold-setting cordierite-based refractory castables were obtained from dead-burnt magnesia, calcined alumina, silica fume, ammonium dihydrogen phosphate, and aggregates in adequate grain size distribution. The paste was easily cast and vibrated, and after heating, a cordierite–mullite composite material was formed.

These phosphate-bonded castables set at room temperature and hardened after a few hours, instead of days, as usually happens with cordieritic materials obtained by a traditional slip-casting method from clays, talc, and/or others.

The MgO-$NH_4H_2PO_4$ bond is suitable for moderate heat duty refractories (below 1250 °C) when a cold set is desired. The phases responsible for the chemical setting and the early strength of the phosphate-bonded castables were mainly ammonium magnesium phosphate hexahydrate (struvite) and amorphous phases. Struvite decomposed at low temperatures, leaving all the phosphates in an amorphous state. On heating at higher temperatures, they crystallized as magnesium orthophosphate and aluminum orthophosphate. At around 1250 °C, cordierite and mullite were formed and the phosphates were believed to remain in the liquid phase.

After calcination at 1350 °C, both conventional- and magnesia–phosphate-bonded castables, have an excellent thermal expansion coefficient (1.3×10^{-6} °C^{-1} and 2.3×10^{-6} °C^{-1}, respectively), making them good for thermal shock services. The magnesia–phosphate-bonded castables exhibit a higher cold and hot flexural strength (13.4 and 14.0 MPa, respectively) than conventional castables (8.1 and 8.1 MPa, respectively).

References

[1] P. Grosjean, Cordierite ceramics, Interceram 42 (1) (1993) 11–15.
[2] S. De Aza, J. Espinosa de los Monteros, Mecanismo de la formación de cordierita en cuerpos cerámicos, Bol. Soc. Esp. Cerám. Vidr. 11 (5) (1972) 315–321.
[3] C. Sorrell, Reaction sequence and structural changes in cordierite refractories, J. Am. Ceram. Soc. 43 (7) (1960) 337–343.
[4] J.L. Mendoza, S. Widjaja, R.E. Moore, Evaluation of cordierite–mullite-bonded kiln furniture refractory saggers, in: R. Fisher (Ed.), Refractory Technology, Ceramic Transactions, vol. 4, American Ceramic Society, Westerville, OH, 1989, pp. 184–204.
[5] A. Goleanu, Synthesizing cordierite in ceramic bodies, Ceram. Ind. 151 (7) (2001) 14–20.
[6] B. Mussler, M. Shafer, Preparation and properties of mullite–cordierite composites, Am. Ceram. Soc. Bull. 63 (5) (1984) 705–710.
[7] Z. Chen, Cordierite self flow castables for kiln furniture, China Refract. 8 (2) (1999) 9–13.
[8] W. Kingery, Fundamental study of phosphate bonding in refractories: I–III, J. Am. Ceram. Soc. 33 (8) (1950) 239–250.
[9] W. Kingery, Fundamental study of phosphate bonding in refractories: IV, J. Am. Ceram. Soc. 35 (3) (1952) 61–63.
[10] P. Gilham-Dayton, The phosphate bonding of refractory materials, Trans. Br. Ceram. Soc. 62 (11) (1963) 895–904.
[11] J. Cassidy, Phosphate bonding then and now, Am. Ceram. Soc. Bull. 56 (7) (1977) 640–643.
[12] J.H. Sharp, H.D. Winbow, Magnesia–phosphate cements, in: P.W. Brown (Ed.), Cement Research Progress, American Ceramic Society, Westerville, OH, 1989, pp. 233–264.
[13] A. Sarkar, Phosphate cement-based fast-setting binders, Am. Ceram. Soc. Bull. 69 (2) (1990) 234–238.
[14] B. El-Jazairi, Rapid repair of concrete pavings, Concrete 16 (9) (1982) 12–15.
[15] B. Abdelrazig, J. Sharp, P. Siddy, B. El-Jazairi, Chemical reactions in magnesia–phosphate cement, Proc. Br. Ceram. Soc. 35 (1984) 141–154.
[16] B. Abdelrazig, J. Sharp, B. El-Jazairi, The chemical composition of mortars made from magnesia–phosphate cement, Cem. Concr. Res. 18 (3) (1988) 415–425.
[17] B. Abdelrazig, J. Sharp, Phase changes on heating ammonium magnesium phosphate hydrates, Thermochim. Acta 129 (1988) 197–215.
[18] B. Abdelrazig, J. Sharp, B. El-Jazairi, The microstructure and mechanical properties of mortars made from magnesia–phosphate cement, Cem. Concr. Res. 19 (2) (1989) 247–258.
[19] S. Popovics, N. Rajendran, M. Penko, Rapid hardening cements for repair of concrete, ACI Mater. J. 84 (1987) 64–73.
[20] S. Popovics, N. Rajendran, Test methods for rapid-hardening magnesium phosphate-based cements, Cem. Concr. Aggreg. 10 (1) (1988) 39–44.
[21] S. Seehra, S. Gupta, S. Kumar, Rapid setting magnesium phosphate cement for quick repair of concrete pavements—Characterisation and durability aspects, Cem. Concr. Res. 23 (2) (1993) 254–266.
[22] D. Hall, R. Stevens, Effect of water content on the structure and mechanical properties of magnesia–phosphate cement mortar, J. Am. Ceram. Soc. 81 (6) (1998) 1550–1556.
[23] Q. Yang, X. Wu, Factors influencing properties of phosphate cement-based binder for rapid repair of concrete, Cem. Concr. Res. 29 (1999) 389–396.
[24] Q. Yang, B. Zhu, S. Zhang, X. Wu, Properties and applications of magnesia–phosphate cement mortar for rapid repair of concrete, Cem. Concr. Res. 30 (2000) 1807–1813.
[25] E. Soudée, J. Péra, Mechanism of setting reaction in magnesia–phosphate cements, Cem. Concr. Res. 30 (2) (2000) 315–321.
[26] T. Sugama, L. Kukacka, Magnesium monophosphate cements derived from diammonium phosphate solutions, Cem. Concr. Res. 13 (3) (1983) 407–416.
[27] T. Sugama, L. Kukacka, Characteristic of magnesium polyphosphate cements derived from ammonium polyphosphate solutions, Cem. Concr. Res. 13 (4) (1983) 499–506.
[28] B. Abdelrazig, J. Sharp, A discussion of the paper on magnesia–phosphate cements by T. Sugama and L.E. Kukacka, Cem. Concr. Res. 15 (5) (1985) 921–922.
[29] T. Finch, J. Sharp, Chemical reactions between magnesia and aluminium orthophosphate to form magnesia–phosphate cements, J. Mater. Sci. 24 (1989) 4379–4386.
[30] J. Ando, T. Shinada, G. Hiraoka, Reaction of monoaluminum phosphate with alumina and magnesia, Yogya Kyokai Shi 82 (1974) 644–649.
[31] E.F. Aglietti, N.E. Hipedinger, A.N. Scian, Cold-setting cordierite castables, in: J.P. Bennett, J.D. Smith (Eds.), Fundamentals of Refractory Technology, Ceramics Transactions, vol. 125, American Ceramic Society, Westerville, OH, 2001, pp. 235–244.
[32] N. Hipedinger, A. Scian, E. Aglietti, Magnesia–phosphate bond for cold-setting cordierite-based refractories, Cem. Concr. Res. 32 (5) (2002) 675–682.